Density of states in graphite from electrochemical measurements on $Li_x(C_{1-z}B_z)_6$

J. R. Dahn and J. N. Reimers
Department of Physics, Simon Fraser University, Burnaby, British Columbia, Canada V5A 1S6

A. K. Sleigh
Moli Energy Ltd., 3958 Myrtle St., Burnaby, British Columbia, Canada V5C 4G2

T. Tiedje
Department of Physics, University of British Columbia, Vancouver, British Columbia, Canada V6T 1Z1
and Department of Electrical Engineering, University of British Columbia, Vancouver, British Columbia, Canada V6T 1Z1
(Received 30 August 1991)

Using electrochemical methods we have measured the variation of the chemical potential μ of intercalated Li in graphite and in boron-substituted graphite as a function of Li concentration x. For small x in $Li_x(C_{1-z}B_z)_6$, μ can be predicted from the density of one-electron levels versus energy, and we find good agreement with the data for pure graphite and for a boron-doped sample. In the rigid-band model, $dx/d\mu$ vs μ is directly proportional to the density of states versus energy, and our measurements of $dx/d\mu$ agree well with empirical tight-binding density-of-states calculations. We show how the values of tight-binding overlap interactions can be *directly* determined from the *electrochemical* data.

INTRODUCTION

Intercalation is observed in a wide variety of materials[1,2] and occurs when the chemical potential μ of the intercalant can be lowered when it enters a solid. For example, Li, K, Rb, and Cs all form intercalation compounds having high concentration with graphite, but Na does not.[3] Presumably, this is because the chemical potential of Na intercalated graphite is larger than at least one of metallic, liquid, or gaseous Na or some Na carbide. Total-energy calculations have not yet reached the stage where accurate estimates of μ at any intercalant composition can be made, so first-principles estimates of the stability of intercalated phases over mixtures of other compounds is currently impossible. The ability to predict and to understand the chemical potential of intercalated species has great consequences in a fundamental understanding of the intercalation process and in the application of intercalation compounds in advanced batteries.

The chemical potential of intercalated Li atoms can be directly measured using electrochemical cells. Generally, these cells have two electrodes, one of metallic Li and one of the intercalation host. The chemical potential of the intercalated Li, μ, with respect to the chemical potential of Li in Li metal is given by $\mu=-eV$, where V is the voltage of the cell (the host is taken as the positive terminal) and e is the magnitude of the electron charge.[4] As the cell is discharged, Li atoms are transferred from the Li-metal anode to the host, where they intercalate. The intercalant composition x is determined from the electrode mass and the charge transferred in the external circuit. If the discharge is done under quasiequilibrium conditions, then measurements of $V(x)$ determine the variation of μ. The reversibility of the intercalation is easily probed by charging the cell.

There have been numerous phenomenological theories used to calculate $\mu(x)$, generally based on lattice-gas models.[5-7] In the simplest of these models the Hamiltonian H includes the binding energy of an isolated Li atom to a site E_0 and interactions between intercalated atoms on sites i and j, U_{ij}:

$$H=\sum_i E_0 x_i+\tfrac{1}{2}\sum_{i,j} u_{ij}x_i x_j \ , \tag{1}$$

where $x_i=1$ or 0 signifies whether a site is occupied or not. Usually E_0 is taken to be a constant (we examine the reasons for this below) and the U_{ij} are restricted to nearest and sometimes next nearest neighbors. These parameters are usually determined empirically by fits to the data, not from first principles. The chemical potential is then obtained from this Hamiltonian using a variety of approximate techniques including mean field theory and Monte Carlo methods. Now we examine the origin of E_0 and U.

When a Li atom is intercalated into a solid, it generally transfers its 2s electron to unoccupied one-electron levels in the host. This chemical bond is what drives the intercalation process and determines the value of E_0. In the rigid-band model, one assumes that the shape of the bands is unchanged by the intercalation and that one-electron levels are filled sequentially as more intercalant is added. In the dilute limit where the intercalated species do not interact, one might expect $\mu(x)$ to match the movement of the Fermi level with respect to the rigid bands. However, the conduction electrons react to the presence of the Li^+ ion and move to screen it. This many-body effect changes the energies of the one-electron eigenstates and makes estimates of $\mu(x)$ difficult. If screening is treated in an elementary way,[8] then as Li is intercalated, the Fermi level moves up with respect to the bands, but the bands move down with respect to the vacuum because of the compensating Li^+ ion. When the

density of states is high, as it is for metallic systems, the downward motion of the bands balances the Fermi level motion and to first order the position of the Fermi level with respect to the vacuum is unchanged. Thus we do not expect E_0 to vary strongly with x for metallic systems, and E_0 can be treated as a constant in Eq. (1).[9] As x increases and more Li^+ ions are intercalated, they interact with one another via screened Coulomb and host-mediated elastic interactions. These interactions are represented by U_{ij} in our model Hamiltonian. Equation (1) has been shown to give a satisfactory description of a variety of intercalation compounds.[5-7]

Selwyn and McKinnon[10] showed that when the Fermi level of an intercalation compound moves through a gap in the density of states, large changes in $\mu(x)$ can result. In this case, the parameter $E_0(x)$ is not constant and changes rapidly with x. The simple approximation of E_0=const, used as a starting point in most lattice-gas treatments of intercalation compounds, then breaks down. If the density of states is low near a gap or in a semimetal, then we expect the Fermi level to move much more rapidly with respect to the bands than the bands move with respect to the vacuum as intercalant is added. Therefore we should be able to predict the variation of $\mu(x)$ near gaps or in semimetals based on the variation of $E_0(x)$ calculated from the density of states and x, neglecting the small band motion caused by the Li^+ ions.

Graphite is a well-known semimetal and is an intercalation compound. We have recently measured $\mu(x)$ for Li intercalated graphite and have determined a phase diagram for the staged phases that form for $x>0.04$ in Li_xC_6.[11] For $x<0.04$, the Li is uniformly distributed in the host and the chemical potential varies more rapidly than can be explained by reasonable choices of U_{ij}. Estimates of the average Li-Li interaction for Li intercalated into graphite give

$$\langle U\rangle=\frac{1}{N}\sum_i U_{ij}=-0.2\ \text{eV}\ ,$$

an attractive interaction, to qualitatively explain the existence of the staged phases and the slope of $V(x)$.[12] For $x<0.04$ the interaction would need to be very large and repulsive (about 10 eV) to explain the rapid decrease of $V(x)$. Therefore we decided to study the effect of the low density of states in graphite on $V(x)$.

Agreement between experiment and theory is better tested when a series of samples with a controlled variable can be studied. In boron-doped graphite, there are valence-band holes, whose number depends on the boron concentration,[13] which must first be filled by transferred electrons as Li is added. These holes have been shown to affect $\mu(x)$,[14] but no quantitative treatment has yet been made.

Here, we present measurements of the voltage of $Li/Li_x(C_{1-z}B_z)_6$ electrochemical cells for graphite and for a boron-doped sample in the range of x, where the intercalated carbon is a single phase with the Li distributed uniformly throughout the host. We compare these measurements with calculations of $V(x)$ based only on the graphite density of states, the boron concentration, and x, finding excellent agreement. Apparently for small x, Li-Li interactions are unimportant, and the variation of $V(x)$ is caused by the motion of the Fermi level with respect to the rigid bands. Finally, we show how tight-binding overlap interaction energies can be extracted from the electrochemical data.

EXPERIMENT

Crystalline synthetic graphite designated KS-44, with an average particle size of 44 μm was obtained from Lonza Corp. (Fair Lawn, New Jersey) and used as received. Boron-substituted synthetic graphite designated as No. 5559 (manufacturer's part number) was obtained from Superior Graphite Co. According to the manufacturer, this material was prepared by heating B_2O_3 and synthetic graphite in the ratio of 1B:10C under N_2 gas using the methods of Lowell.[15] During heating, oxygen reacts with the carbon and is released as CO_2. According to the B-C phase diagram,[15] this could result in boron-substituted graphite with $z=0.0235$ in $C_{1-z}B_z$ and a small amount of B_4C. The addition of B_4C does not affect our electrochemical measurements apart from a correction for inactive mass since B_4C does not intercalate Li.[16] It is difficult to measure the boron concentrations directly. Chemical-analysis techniques do not distinguish B as B_4C from boron substituted into graphite. The lattice constants of boron-doped graphite do vary with boron concentration,[15] but the variation is small on the scale of the variation expected in pure graphitic carbons due to changes in heating conditions and changes in the amount of disorder in the carbon.[17] Therefore, we do not have a good experimental determination of the number of boron atoms substituting for carbon atoms in the No. 5559 sample, although we will see below that the agreement between experiment and theory is good if $z=0.0062$.

$Li/Li_x(C_{1-z}B_z)_6$ electrochemical cells were constructed as described elsewhere.[12,18] We used a solution of 1 M $LiN(CF_3SO_2)_2$ and 1 M 12-crown-4 ether dissolved in a 50:50 volume mixture of propylene carbonate and ethylene carbonate for the electrolyte in the cells reported here. $LiN(CF_3SO_2)_2$ was obtained from 3M Corporation and was vacuum dried at 140 °C prior to use. 12-crown-4 ether was obtained from Aldrich Chemical Co. and was used as received. Propylene carbonate and ethylene carbonate were obtained from Texaco and were vacuum distilled before use. The moisture content of the electrolyte was less than 100 ppm by weight. To make electrodes, the powdered carbons were mixed with a 4% ethylene propylene diene monomer (EPDM) solution in cyclohexane and excess cyclohexane to make a slurry with a syrupy viscosity. The amount of EPDM was chosen so that 2% by weight of the finished electrode would be EPDM. The slurry was then spread using a doctor-blade spreader onto a copper-foil substrate, and the cyclohexane was evaporated. Electrodes were then pressed between flat plates with a pressure of 10 MPa. Typical electrodes were 150 μm thick with a mass density of 15 mg/cm^2.

To determine $V(x)$ and its derivative $-dx/dV$, cells were charged and discharged using constant currents between fixed voltage limits. The temperature of the cell

was maintained constant in a thermostat to ±0.1 °C. The cell cyclers maintain stable currents to ±0.5%. Changes in x are calculated from the cathode mass, the constant current, and the time of the current flow. Data were measured whenever V changed by ±0.005 V. The derivative, $-dx/dV$ is calculated by taking differences between adjacent data points.

THEORY

According to previous work,[19] the Fermi level of graphite moves by about 1.3 eV with respect to the bands as Li is intercalated all the way to the composition limit. Only the π bands of graphite, derived from the carbon $2p_z$ orbitals, fall in this range. If we use the rigid-band model, assume complete charge transfer from the Li to the host, and assume each substitutional boron atom can be treated as a carbon with one less valence electron, then we only need include the π bands in our calculation. We used two simple methods to calculate the density of states, one based on Harrison's universal linear combination of atomic orbital (LCAO) theory[20] and the other on an analytic expression for the density of states near the Fermi level due to Wallace.[21] The latter method is also based on the empirical tight-binding method. We include an orbital overlap interaction between $2p_z$ orbitals on nearest-neighbor carbon atoms on the same layer and between $2p_z$ orbitals on nearest-neighbor carbon atoms in adjacent layers. In Harrison's notation these overlaps are $V_{pp\pi}$ and $V_{pp\sigma'}$, respectively, where the prime represents an interlayer interaction. In Wallace's notation, these overlaps are γ_0 and γ_1, respectively. For simplicity, we will adopt Wallace's notation here.

Figure 1 compares the π-band density of states of graphite calculated near the Fermi level using the two methods described above for $\gamma_0=2.66$ eV and $\gamma_1=0.4$ eV. These parameter choices are near currently popular values,[22] and the dispersion for the π bands reproduces well that from more sophisticated theories.[23] The spin degeneracy has been included in the results. For the LCAO method we evaluated the four eigenvalues at 330 000 points in the first Brillouin zone and calculated the density of states in the normal way[20] using a histogram binning interval of 50 meV. Because the analytic expressions agree well with the LCAO within 1 eV of the Fermi level, we used them in our calculations of the variation of the chemical potential μ of intercalated Li with Li concentration x to be described next.

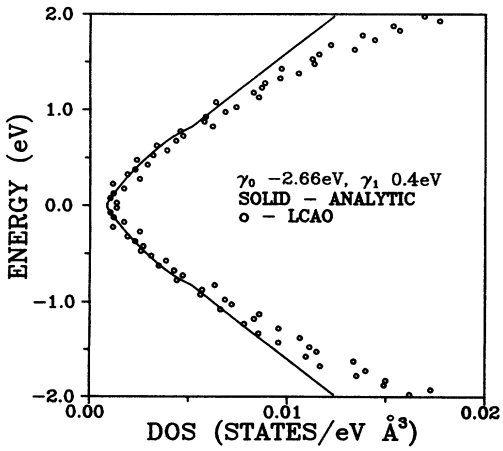

FIG. 1. Density of one-electron levels vs energy near the Fermi level of graphite, calculated using LCAO and using the analytic expression given in Eq. (4).

For simplicity, we work at zero temperature for the electrons. We define $E_f(x,z)$ to be the position of the Fermi level in $\mathrm{Li}_x(\mathrm{C}_{1-z}\mathrm{B}_z)_6$ such that $E_f(0,0)=0.0$ eV. Then, for small x and z, using the rigid-band model,

$$z=\tfrac{1}{4}\int_{E_f(0,z)}^{E_f(0,0)} N(E)dE \tag{2}$$

and

$$x=\tfrac{3}{2}\int_{E_f(0,z)}^{E_f(x,z)} N(E)dE\ , \tag{3}$$

where $N(E)$ is the density of one-electron levels per unit energy per graphite unit cell (four atoms per unit cell). The factor of $\frac{3}{2}$ in Eq. (3) is due to our convention of specifying x as x in $\mathrm{Li}_x(\mathrm{C}_{1-z}\mathrm{B}_z)_6$, and the number of atoms per cell, giving $\frac{6}{4}$. We use the form of $N(E)$ from Haering and Wallace [Ref. 24, their Eq. (2.5)]:

$$N(E)=\frac{4}{3^{1/2}\pi^2\gamma_0^2}\left[(4\gamma_1^2-E^2)^{1/2}+\pi|E| +2E\sin^{-1}\left[\frac{E}{2\gamma_1}\right]\right] \quad \text{for } E\le|2\gamma_1| \tag{4a}$$

and

$$N(E)=\frac{8}{3^{1/2}\pi\gamma_0^2}|E| \quad \text{for } E\ge|2\gamma_1|\ . \tag{4b}$$

The chemical potential $\mu(x,z)$ of the intercalated Li is then

$$\mu(x,z)=E_f(x,z)+E_0+kT\ln[x/(1-x)]\ , \tag{5}$$

where E_0 is a constant, k is Boltzmann's constant, and T is the Kelvin temperature. The last term in (5) includes the configurational entropy associated with arranging xN Li ions randomly on N sites. We showed that for small x, the Li is uniformly distributed through the host[11] so this entropy term is approximately correct. Since x is small, this entropy term can be several kT so we must include it, even though we have neglected the effects of temperature in calculating the Fermi level position where the error will be less than kT (at room temperature, $kT\cong0.025$ eV). The voltage $V(x,z)$ of the $\mathrm{Li}/\mathrm{Li}_x(\mathrm{C}_{1-z}\mathrm{B}_z)_6$ cell is then given by

$$V(x,z)=-\mu(x,z)/e\ . \tag{6}$$

We use Eqs. (2), (3), and (4) to solve for E_f as a function of x and z and Eqs. (5) and (6) to obtain V. The derivative $-dx/dV$ is obtained from V by differentiating (6). If the effects of temperature are neglected [omit the last term in (5)], then

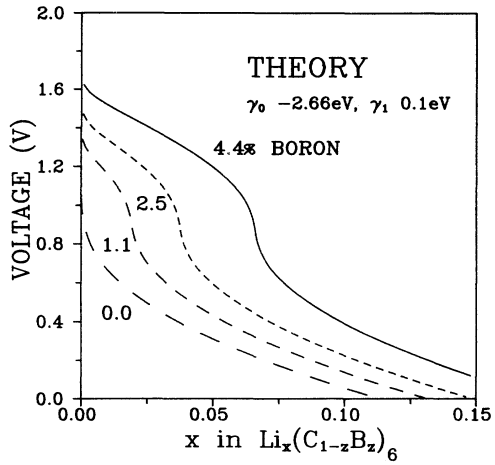

FIG. 2. Variation of the voltage of $Li/Li_x(C_{1-z}B_z)_6$ electrochemical cells with x for several boron concentrations as predicted by the theory described in the text. The boron concentration in atomic percent is indicated next to each curve.

$$\frac{-dx}{dV}=1.5eN(E_f(x,z)) \ . \tag{7}$$

Therefore, $-dx/dV$ versus cell voltage is a measure of $N(E)$ as a function of E *subject* to the constraints that the density of states is low so that the rigid-band model can be used.

The value of $-dx/dV$ when the Fermi level coincides with the minimum in the density of states ($E_f=0$ in our formalism) is easily found using Eq. (4),

$$\frac{-dx}{dV}(E_f=0)=\frac{4\sqrt{3}\gamma_1}{\pi^2\gamma_0^2}e \ , \tag{8}$$

where the unit of $-dx/dV$ is V^{-1}. Therefore measurements of $-dx/dV$ allow a direct measurement of the ratio of overlap interactions. Notice that Eq. (8) is independent of z so that comparisons with theory are possible for samples having unknown boron concentration.

Figure 2 shows $V(x)$ calculated for several values of z using $E_0=-0.8$ eV. The effect of the added boron is clearly seen as the formation of the upper plateau (near 1.2 V), which grows in length as boron is added. The sharp drop in voltage occurs as the Fermi level passes

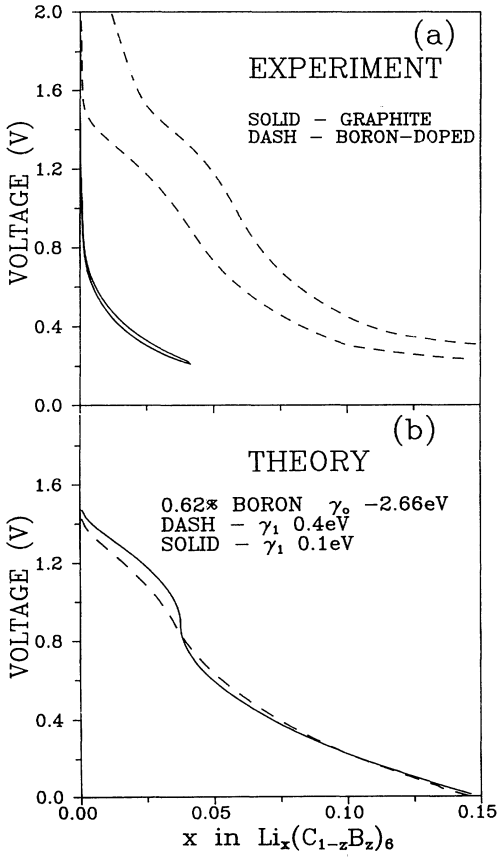

FIG. 3. Voltage vs x for $Li/Li_x(C_{1-z}B_z)_6$ cells. (a) Experiment for graphite and for the boron-doped sample. The lower curve for each set of data was measured during the discharge of the cell (intercalating Li) and the upper curve for the charge (removing Li). (b) Theoretical curves showing that $\gamma_1\cong 0.4$ eV is needed to explain the smoothness of $V(x)$ for the boron-doped sample.

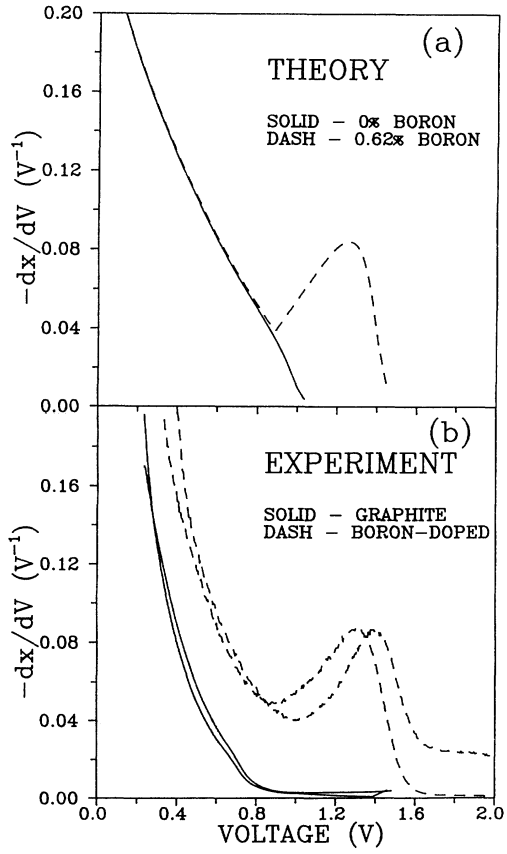

FIG. 4. The derivative $-dX/dV$ plotted vs V for $Li/Li_x(C_{1-z}B_z)_6$ cells. (a) Theoretical curves as described in the text. (b) Experimental results; the left-hand curve for each compound was measured during the discharge of the cell and the right-hand curve for the charge of the cell.

through the minimum in the density of states. The position of this drop, x_d, can be used to directly measure the boron concentration in the sample since $z = x_d/6$. Now we test the agreement between experiment and theory.

RESULTS AND DISCUSSION

Figure 3(a) shows the voltage versus x for $Li/Li_x(C_{1-z}B_z)_6$ cells with electrodes of pure graphite and of the boron-doped sample, which agree qualitatively with the theoretical curves shown in Fig. 2. The cell with the graphite electrode was cycled using currents that corresponded to a change $\Delta x = 1$ in 400 h (we call this a 400-h rate), while the cell with the boron-containing electrode was cycled using an 80-h rate. The offset between charge and discharge curves in the figure is caused by the voltage drop in the internal impedance of the cell. (The internal impedance is dominated by mass transport terms including the diffusion of the Li^+ ions in the liquid electrolyte and solid-state diffusion of the intercalated Li.) The graphite cell was only discharged to 0.230 V; below this voltage, staged phases begin to form.[11] The boron-containing cell gives a short plateau in $V(x)$ near 1.2 V, which is due to the addition of the boron but the drop in voltage near 0.8 V is not nearly as sharp as those shown in Fig. 2. Figure 3(b) shows the effect of changes in γ_1 on the sharpness of the drop in $V(x)$. For $\gamma_1 = 0.4$ eV, using $z = 0.0062$, the theory is in good agreement with the data.

A more critical comparison is possible when $-dx/dV$ is compared to the predictions of theory, as is done in Fig. 4. Figure 4(a) shows the theoretical predictions using $\gamma_1 = 0.4$ eV for $z = 0$ and $z = 0.0062$, using $E_0 = -0.8$ eV. The experimental data in Fig. 4(b) for graphite and for the boron-doped sample agrees very well with the theory apart from the offset between the curves below 0.8 V which we will return to below. We can use Eq. (8) to calculate the minimum in $-dx/dV$; for the parameters shown we get 0.040 V^{-1} in excellent agreement with the data for the boron-doped sample. Alternatively we could use our measurements to extract the ratio $\gamma_1/(\gamma_0^2)$.

We have used the rigid-band model to describe the changes in the chemical potential of the intercalated Li and have totally ignored the effects of the compensating positive charge. We have also ignored the fact that the binding energy for $2p$ electrons is lower for boron than it is for carbon.[20] The effect of the boron is to move the π bands up slightly with respect to the vacuum. In the simplest model,[9] the added Li ions cause the bands to move down as more intercalant is added. The data in Fig. 4(b) compare $-dx/dV$ for two values of z at the same voltage, *not* at the same x. The boron-substituted carbon has more Li added at any voltage, so the offset between $-dx/dV$ for graphite and for the boron-doped sample is due to the motion of the bands caused by the Li^+ ions and the added boron. The data in Fig. 4(b) show that the bands move down by about 0.3 eV for $z = 0.0062$ and $x \cong 0.05$ relative to their position for $x = z = 0$.

We have shown that the variation of the chemical potential of Li in Li intercalated graphite and in boron-substituted graphite can be well predicted using the rigid-band model provided the intercalant concentration is low enough so Li-Li interactions can be ignored. Our theory has no adjustable parameters since it depends only on the graphite band structure and agrees well with the data. In fact, the overlap interactions used as parameters in the tight-binding theory are directly measurable from the electrochemical data. These results clearly show that electronic structure considerations are important in calculations of the variation of the chemical potential of intercalated species, especially when the density of states is small.

[1] S. A. Solin, in *Advances in Chemical Physics,* edited by I. Prigogine and S. A. Rice (Wiley, New York, 1982), Vol. XLIX.

[2] M. S. Whittingham, Prog. Solid State Chem. **12**, 41 (1978).

[3] D. P. DiVincenzo and E. J. Mele, Phys. Rev. B **32**, 2538 (1985).

[4] W. R. McKinnon and R. R. Haering, in *Modern Aspects of Electrochemistry,* edited by R. E. White, J. O'M. Bockris, and B. E. Conway (Plenum, New York, 1983), Vol. 15.

[5] J. R. Dahn and W. R. McKinnon, J. Phys. C **17**, 4231 (1984).

[6] S. T. Coleman, W. R. McKinnon, and J. R. Dahn, Phys. Rev. B **29**, 4147 (1984).

[7] R. Osorio and L. M. Falicov, J. Phys. Chem. Solids **43**, 73 (1982).

[8] J. Friedel, Adv. Phys. **3**, 446 (1954).

[9] W. R. McKinnon, in *Chemical Physics of Intercalation,* edited by A. P. Legrand and S. Flandrois (Plenum, New York, 1987), p. 181.

[10] L. S. Selwyn and W. R. McKinnon, J. Phys. C **20**, 5105 (1987).

[11] J. R. Dahn, Phys. Rev. B **44**, 9170 (1991).

[12] J. R. Dahn, Rosamaria Fong, and M. J. Spoon, Phys. Rev. B **42**, 6424 (1990).

[13] S. Marinkovic, in *Chemistry and Physics of Carbon,* edited by P. A. Thrower (Dekker, New York, 1984), Vol. 19.

[14] J. R. Dahn, J. N. Reimers, T. Tiedje, Y. Gao, A. K. Sleigh, W. R. McKinnon, and S. Cramm (unpublished).

[15] C. E. Lowell, J. Am. Ceramic Soc. **50**, 142 (1967).

[16] A. K. Sleigh (unpublished).

[17] W. Ruland, Acta Crystallogr. **18**, 992 (1965).

[18] Rosmaria Fong, U. Von Sacken, and J. R. Dahn, J. Electrochem. Soc. **137**, 2009 (1990).

[19] W. Eberhardt, I. T. McGovern, E. W. Plummer, and J. E. Fischer, Phys. Rev. Lett. **44**, 200 (1980).

[20] W. A. Harrison, *Electronic Structure and the Properties of Solids* (Freeman, San Franscisco, 1980).

[21] P. R. Wallace, Phys. Rev. **71**, 622 (1947).

[22] Y. Yoshida and S. Tanuma, Synth. Metals **23**, 199 (1988).

[23] N. A. W. Holzwarth, S. G. Louie, and S. Rabii, Phys. Rev. B **26**, 5382 (1982).

[24] R. R. Haering and P. R. Wallace, in *Proceedings of the 1957 Conference on Carbon,* edited by S. Mrozowski, M. L. Studebaker, and P. L. Walker (Pergamon, New York, 1957), p. 183.